View Article Online / Journal Homepage / Table of Contents for this issue

Published on 04 July 2011. Downloaded by University of California - Santa Cruz on 29/10/2014 23:10:02.

This article is published as part of the *Dalton Transactions* themed issue entitled:

Pincers and other hemilabile ligands

Guest Editors Dr Bert Klein Gebbink and Gerard van Koten

Published in issue 35, 2011 of *Dalton Transactions*

Image reproduced with permission of Jun-Fang Gong

Articles in the issue include:

PERSPECTIVE:

ARTICLES:

Visit the *Dalton Transactions* website for more cutting-edge inorganic and organometallic research
www.rsc.org/dalton

Dalton Transactions

Dynamic Article Links

Cite this: *Dalton Trans.*, 2011, **40**, 8796

www.rsc.org/dalton

PAPER

Published on 04 July 2011. Downloaded by University of California - Santa Cruz on 29/10/2014 23:10:02.

Aryl–O reductive elimination from reaction of well-defined aryl–Cu^{III} species with phenolates: the importance of ligand reactivity†

Alicia Casitas,[a] Nikolaos Ioannidis,[b] George Mitrikas,*[b] Miquel Costas[a] and Xavi Ribas*[a]

Received 14th March 2011, Accepted 12th April 2011
DOI: 10.1039/c1dt10428d

Well-defined aryl–Cu^{III} species undergo rapid reductive elimination upon reaction with phenolates (PhO^-), to form aryl–OPh cross-coupling products. Kinetic studies show that the reaction follows a different mechanistic pathway compared to the reaction with phenols. The pH active cyclized pincer-like ligand undergoes an initial amine deprotonation that triggers a faster reactivity at room temperature. A mechanistic proposal for the enhanced reactivity and the role of EPR-detected Cu^{II} species will be discussed in detail.

Fundamental mechanistic knowledge of the relevant redox steps in Cu-catalyzed Ullmann-type aryl–heteroatom cross-coupling chemistry is still scarce.[1–4] These classic reactions have gained renewed interest due to cost and toxicity benefits in comparison to Pd-based methodologies for the synthesis of key intermediates in the pharmaceutical industry.[5,6] Focusing in the copper-based cross-coupling reactions to form aryl–O bonds,[7] we have recently reported a detailed mechanistic investigation on the reactivity of well-defined aryl–Cu^{III} species system with HO-nucleophiles (HO-Nuc). These reactions afford corresponding aryl-*O*-Nuc products under mild conditions, *via* a reductive elimination path.[8] The aryl–Cu^{III} species (complex **2**) under study has been synthesized by copper(II) metallation at the aromatic ring of the triazamacrocyclic ligand (**1**) *via* a disproportionation pathway.[9,10] Interestingly, ligand **1** can be considered as a cyclized evolution of typical NCN-pincer-like complexes, that are usually prepared by metallation with 2nd and 3rd row transition metals, more prone to direct C–H activation.[11] The cyclized ligand **1** thus shows the ability of coordinating a first row transition metal ion such as Cu or Ni in close proximity to the aromatic C–H bond. This feature enables easy C–H bond cleavage under very mild conditions (Scheme 1).[9]

Furthermore, increasing interest is devoted to reactivity with multifunctional ligands that are not mere spectators, but on the contrary, that respond to effects such as changes in pH.[12] In this paper we show a diverse reactivity of the cyclized pincer-like complex **2**, in response to the nucleophile Brønsted base nature; the reaction of **2** with different *para*-substituted sodium phenolate (*p*X-PhONa) substrates substantially differs from that

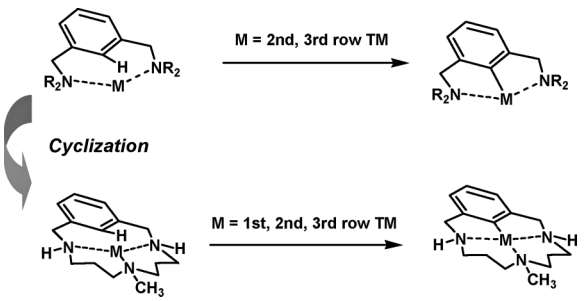

Scheme 1

with the corresponding phenols, despite both type of reactions afford the same biaryl ether products.[8] Unlike reactions with phenols, for which reaction intermediates are not observed, and are kinetically described as simple bimolecular **2**/HO-Nuc reactions, the reaction of **2** with phenolates involves formation of a purple intermediate solution and a notable enhancement of aryl–OPh formation reaction rates. The chemical nature of the reaction intermediates, as well as the pH-non-innocence role of the ligand is discussed.

The reaction of **2** with equimolar amounts of several sodium phenolates was monitored by UV-vis spectroscopy. Phenolate addition caused the instantaneous formation of a deep-violet species **3** ($\lambda_{max} = 545$ nm, $\varepsilon = 2040$ M^{-1} cm^{-1}). Compound **3** decayed without accumulation of any additional intermediate species, affording the corresponding aryl–O biaryl ethers in quantitative yields (Fig. 1 and Table 1), as ascertained by ^{1}H NMR, UV-vis and ESI-MS. The formation of the violet species **3** is not observed for the reaction of **2** with the corresponding phenols.[8] In addition, species **3** decays faster than complex **2**, upon reaction with phenol substrates (Fig. 2), under analogous experimental conditions. The latter observations suggest that the two reactions occur through distinct mechanistic pathways, albeit for the obtention of the same biaryl ether and Cu^I final products. When a series of *p*X-PhONa were employed as nucleophiles, relative reaction rates correlate

[a]*Departament de Química, Universitat de Girona, Campus de Montilivi, 17071, Girona, Catalonia, Spain. E-mail: xavi.ribas@udg.edu; Fax: +34-972418150; Tel: 972-418262*
[b]*Institute of Materials Science, NCSR "Demokritos", 15310, Athens, Greece. E-mail: mitrikas@ims.demokritos.gr; Fax: + (30-210-6503381); Tel: +(30-210-6503304)*

† Electronic supplementary information (ESI) available: Experimental details. See DOI: 10.1039/c1dt10428d

This journal is © The Royal Society of Chemistry 2011

Published on 04 July 2011. Downloaded by University of California - Santa Cruz on 29/10/2014 23:10:02.

Table 1 Reactivity of complex **2** with 1 equiv. of *p*-X-phenolate substrates (X = OCH_3, Cl, F, CN and NO_2) to afford the corresponding biaryl ethers ([**2**] = 1.2 mM, 25 °C, N_2 atmosphere). The reactivity of **2** with three corresponding phenols is included for comparison

Substrate	Time (min)	Aryl–O product yield (%)
p-OCH_3-phenolate	10	100
p-OCH_3-phenol	100	100
p-F-phenolate	25	100
p-F-phenol	200	100
p-CN-phenolate	15	100
p-CN-phenol	125	100
p-NO_2-phenolate	—	100[a]
p-Cl-phenolate	—	100[a]

[a] [**2**] = 0.6 mM, T = 10 °C.

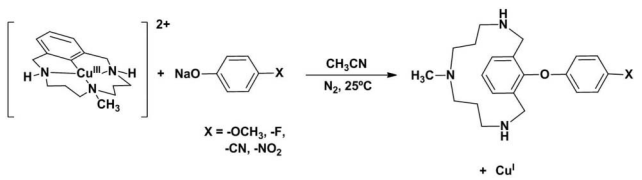

Fig. 1 Reaction of **2** with a family of *para*-substituted phenolates (Na salt) to afford the corresponding biaryl ether coupling products and Cu^{I}.

with the electronic nature of X, and electron withdrawing groups provide the fastest reaction rates (see Fig. S4†).

Mechanistically, the aryl–O coupling reaction between **2** and phenols consists of a reductive elimination from a transient, spectroscopically and kinetically detected aryl–Cu^{III}–(phenol) species (*i.e.* for *p*CN-phenol) to afford corresponding biaryl ethers and Cu^{I}.[8] On the contrary, the distinct formation of the violet species **3** upon reaction of **2** with *p*X-PhONa, as well as the substantially faster reaction rates observed, prompted us to undertake a detailed study in order to gain more insight into the mechanistic pathway. The first question to resolve was the identity of species **3**. UV-vis analysis show that the UV-vis spectroscopic features of **3**, prepared by reaction with 1 equiv. *p*X-PhONa (X = OCH_3, Cl, F, CN and NO_2), are the same, irrespective of the nature of *p*X-PhONa. On the other hand, the addition of bases such as Et_3N or Proton Sponge® also caused the formation of **3**, albeit up to 5–7 equiv. of the base were necessary for full formation of **3** (see Supp Info†). Furthermore, the reaction of **2** with Proton Sponge® followed by the addition of 1 equiv. of *p*F-phenol renders exactly the same decay profile, monitored at λ = 545 nm, to the one observed for the reaction with 1 equiv. of *p*F-PhONa (Fig. 2a). Altogether, the data suggest that complex **2** suffers a deprotonation of one of the secondary amines (Scheme 2). In this regard, the intense violet chromophore may tentatively be assigned to LMCT transitions from the amido N to the Cu^{III} center. Indeed, similar UV-vis spectroscopic features have been described by Margerum and co-workers to arise after amine deprotonation in Cu^{III}–peptide complexes.[13–15]

In order to prove the reversibility of this reaction we conducted a UV-vis experiment to monitor the spectrum upon subsequent addition of *p*F-phenolate and triflic acid (Fig. 3). The experiment was performed at –30 °C to minimize evolution of **3** towards the formation of the aryl–O product. The addition of *p*F-PhONa causes the instantaneous formation of species **3**, and subsequent addition of triflic acid restores complex **2**. The phenolate/acid

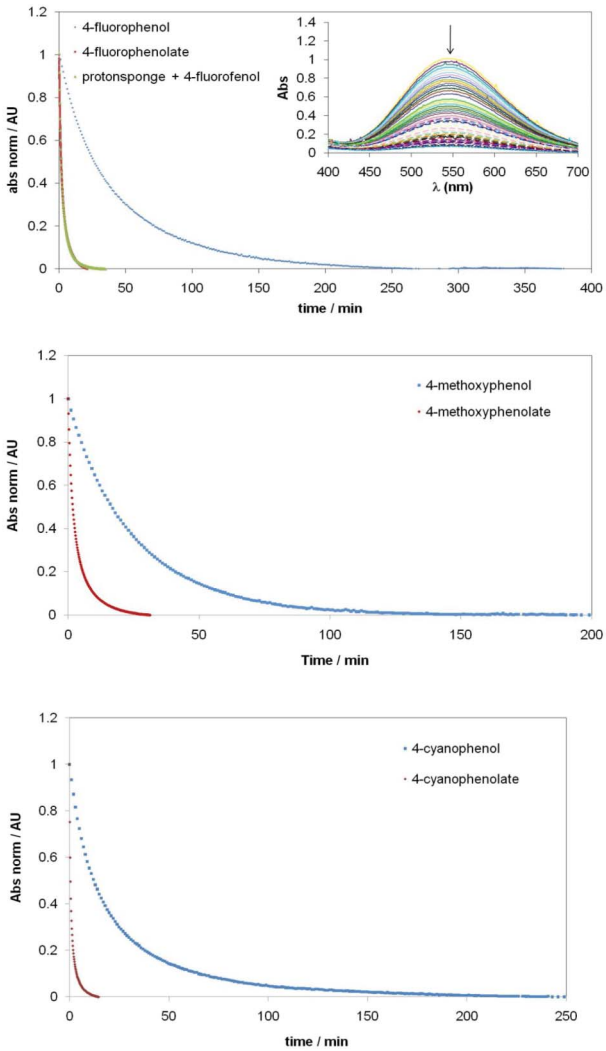

Fig. 2 Decay profiles (abs normalized *vs.* time) for the 550 nm band for the reaction of equimolar amounts of **2** and different *p*X-PhONa (and corresponding phenols): (a) 1 equiv. *p*F-PhONa; 1 equiv. *p*F-PhOH (inset: 550 nm band decay); 3 equiv. Proton Sponge® + 1 equiv. *p*F-PhOH; (b) 1 equiv. *p*MeO-PhONa; 1 equiv. *p*MeO-PhOH; and (c) 1 equiv. *p*CN-PhONa; 1 equiv. *p*CN-PhOH. (Conditions: [**2**] = 1.2 mM, 25 °C, N_2 atmosphere.)

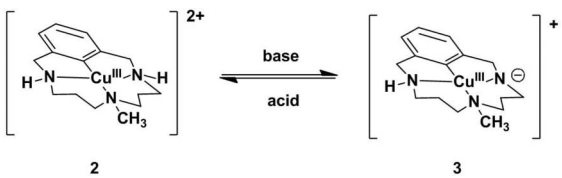

Scheme 2

cycle can be repeated several times, and only a minor loss of 6% for complex **2** (at 450 nm) is observed after 3 cycles. Similarly, the recovery of complex **3** after three cycles is up to 94%. The minor decomposition observed may be caused by ongoing formation of the aryl–O coupling product.

The equimolar reaction of **2** and sodium *p*F-phenolate to form **3** was monitored by ^{1}H NMR at –30 °C (Supp. Info†). The addition of 1 equiv. of *p*F-PhONa caused important changes in

Published on 04 July 2011. Downloaded by University of California - Santa Cruz on 29/10/2014 23:10:02.

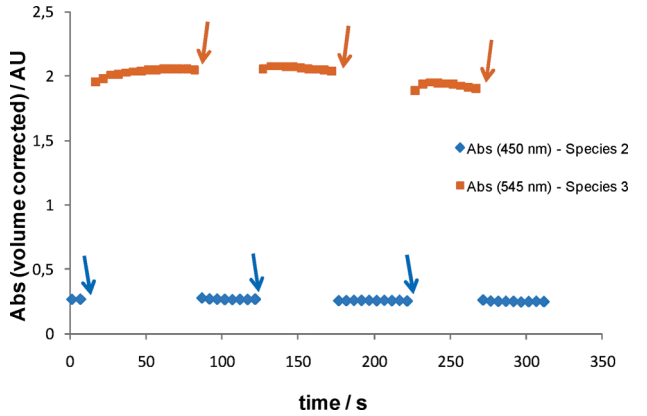

Fig. 3 UV-vis monitoring of the consecutive additions of 1 equiv. of *p*F-PhONa and triflic acid to a solution of **2**. Blue arrows indicate addition of phenolate; orange arrows indicate addition of triflic acid. $[\mathbf{2}]_{initial} = 1$ mM, –30 °C.

the spectrum with respect to that of the diamagnetic Cu^{III} species **2**: signals corresponding to protons nearby the deprotonated secondary amine group showed a broadening (benzylic CH_2 at 4.25 ppm; α-CH_2 at 2.95 ppm), whereas the rest of the signals remained unmodified. Similarly, when species **3** was generated with a base (6 equiv. of Proton Sponge® at –30 °C), the same signals were affected (Supp. Info†). Indeed, the same signals suffered slight up-field shifts and further broadening upon gradual warming up to 20 °C, but the initial spectrum was recovered if the solution was cooled back to low temperature. Bi-dimensional correlations indicated also the disappearance of ^{13}C peaks corresponding to the affected CH_2 moieties in **3**. A reasonable explanation to these observations is that amine deprotonation allows for different conformations (flipping) at the deprotonated amine, giving rise to a severe broadening effect of the α-CH_2 signals.

A low temperature ^1H NMR experiment corresponding to the reaction of **2** with *p*F-PhONa also showed that species **3** is not stable and gradual fading of the signals assigned to **3** was observed, along with the growth of signals corresponding to *p*F-OPh-aryl coupling product (Fig. S10†). No accumulation of other intermediate species was observed along this transformation. Signals corresponding to **3** account for ~90% of complex mass balance, and thus we suspected that another NMR silent copper-containing species, namely **3′**, could be present.

The chemical nature of species **3′** is unclear. We conducted an extensive cw and pulse-EPR study to shed some light into its chemical nature. Reaction samples of **2** (44 mM) and 4 equiv. of Proton Sponge® were mixed under N_2 at 0 °C, stirred for a few seconds and immediately frozen in an EPR tube. X-band (9.4 GHz) and Q-band (34.6 GHz) measurements were performed at T = 120 K (see Fig. 4). The EPR spectra in both mw frequencies can be satisfactorily simulated with the following spin Hamiltonian parameters: $g_x = 2.0384$, $g_y = 2.0215$, $g_z = 2.1147$; $A_x = 124$ MHz, $A_y = 447$ MHz, $A_z = 134$ MHz. Although g and A tensors are typical for $S = \frac{1}{2}$ Cu^{II} species, the orientation of the tensors is unusual: the large hyperfine value 447 MHz is along g_y and not g_z, as is the case for most common Cu^{II} EPR signals. However, this behavior can be rarely found in the literature.[16] For instance, wild-type *stellacyanin*, a blue copper protein, shows a roughly axial hyperfine tensor A, but the largest hyperfine splitting (hfs) is along

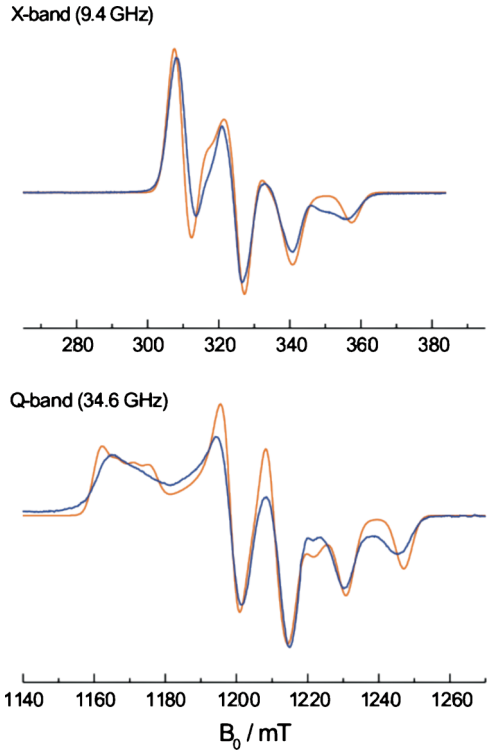

Fig. 4 X- and Q-band EPR spectra of **3** in frozen acetonitrile solution (T = 120 K). Blue traces: experiment; orange traces: simulation. For simulation parameters see text.

the minimum g value, that is assigned to a tetrahedral or nearly tetrahedral geometry for Cu^{II}.[17–19]

Some insight about the atoms surrounding the Cu^{II} ions could be obtained by ENDOR and HYSCORE spectra (see Supp. Info†). The ENDOR study showed two strongly-coupled nitrogen atoms, with A = 12 MHz and A = 46 MHz hyperfine coupling constants, respectively. Additionally, HYSCORE spectra allowed for the detection of a third weakly (A = 4 MHz) coupled N atom. The latter findings could be tentatively rationalized with a Cu^{II} coordination sphere consisting of two strongly bound amine moieties, as well as a third weakly coordinated N belonging to a CH_3CN molecule. Since a tetrahedral geometry is deduced from spin Hamiltonian parameters, and the macrocyclic ligand appears incapable of adapting to this geometry, while keeping the four N atoms bound to the metal, an external CH_3CN ligand is proposed to be bound to the metal center, leaving one of the macrocylic secondary amine groups as non-coordinated. Moreover, spectra also showed the existence of two weakly coupled protons, one at A_1 = 6 MHz and another one at A_2 = 14 MHz with modest anisotropy (agreement between ENDOR and HYSCORE). An additional proton coupling with considerable anisotropy is found, with a short $Cu^{II} \cdots H$ distance of 2.34 Å (assuming a 100% spin density at Cu^{II}).

Despite the uncertainty on the nature of **3′**, since it is a $S = \frac{1}{2}$ system, we could perform a reliable quantification by comparison with the signal of a well-characterized $Cu^{II}(acac)_2$ complex (see Supp. Info†). We noticed that the formation of the EPR active species **3′** is only about the 2% of the starting copper content for base treatment of low concentration of **2**, whereas it increases up to 11% for higher concentrations of **2**.

 This journal is © The Royal Society of Chemistry 2011

Published on 04 July 2011. Downloaded by University of California - Santa Cruz on 29/10/2014 23:10:02.

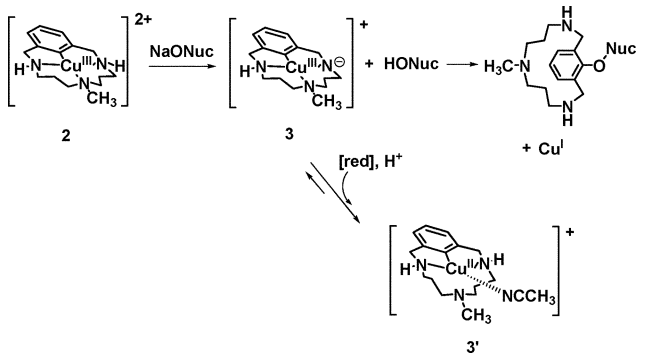

Fig. 5 Proposed mechanism for the reactivity of aryl–Cu^{III} species **2** with *p*X-phenolates (sodium salt).

Given the above reported data, we can tentatively propose the mechanism depicted in Fig. 5 for the equimolar reaction of **2** with *p*X-PhONa. The first step consists of the deprotonation of one secondary amine by the basic phenolate to yield **3** and the corresponding phenol. At this point, deprotonated Cu^{III} complex **3** interacts with *in situ* formed phenol substrate and undergoes reductive elimination to form the final aryl–O and Cu^{I} products. This reaction is much faster than that of complex **2** with phenols. The proposal of a reductive elimination step is consistent with several examples in the literature of reactions between well-defined aryl–Cu^{III} species and N- and O-nucleophiles,[8,20,21] as well as with aryl-halide reductive elimination examples at well-defined aryl–Cu^{III}-halides.[22] Furthermore, reductive elimination at aryl–Cu^{III} species is also proposed in mechanistic studies on Ullmann-like coupling reactions.[4,7,23,24]

In addition, in a side reaction (2–11%), **3** can undergo 1e^{-} reduction to form an aryl–Cu^{II}N$_3$ species **3′** with a tetrahedral coordination geometry. The origin of the e^{-} could not be ascertained, but possible sources could be Cu^{I}, PhOH and PhO^{-} species, all of them present in the reaction mixture. Whatever its origin, since aryl–ONuc products are obtained in quantitative yield, we conclude that **3′** is also consumed in the reaction, and that side reactivity of **3** to form **3′** must be reversible.

Summarizing, we have demonstrated that the reactivity of well-defined aryl–Cu^{III} species in front of phenol-type nucleophiles differs substantially from the reactivity with corresponding phenolates, and a significant enhancement is found to produce the same aryl–O coupling product. Mechanistic studies show that easy deprotonation of coordinated secondary amines is responsible of the intense LMCT band at 545 nm; indeed, this pH-dependent reactivity of the pincer-like coordinated ligand somewhat enhances its reactivity. The origin of such enhancement is not clearly understood, and is currently been studied computationally. A parallel reaction path for deprotonated species **3** affords minor quantities of an EPR-active species **3′**. The present observations of a substantial enhancement in the cross-coupling reactivity observed upon ligand deprotonation suggests that this might be a strategy to take into account in the design of more efficient Cu^{III}-mediated C–heteroatom bond-forming reactions.

We thank S. S. Stahl and L. M. Huffman for fruitful discussions. We also thank T. Parella for help on the NMR analysis. We acknowledge financial support from the MICINN of Spain (CTQ2009-08464/BQU to M.C. and CTQ2008-03077/BQU to M.S.), the DIUE of Catalonia (2009SGR637). A.C. thanks MICINN for a PhD grant. M.C. and X.R. thank Generalitat de Catalunya for ICREA Academia Awards and 2009 SGR637. We also thank STR-UdG for NMR and ESI-MS technical support.

Notes and references

1 I. Goldberg, *Ber. Dtsch. Chem. Ges.*, 1906, **39**, 1691–1696.
2 F. Ullmann, *Ber. Dtsch. Chem. Ges.*, 1903, **36**, 2389.
3 F. Ullmann and J. Bielecki, *Chem. Ber.*, 1901, **34**, 2174.
4 E. Sperotto, G. P. M. v. Klink, G. v. Koten and J. G. d. Vries, *Dalton Trans.*, 2010, **39**, 10338–10351.
5 I. P. Beletskaya and A. V. Cheprakov, *Coord. Chem. Rev.*, 2004, **248**, 2337–2364.
6 G. Evano, N. Blanchard and M. Toumi, *Chem. Rev.*, 2008, **108**, 3054–3131.
7 F. Monnier and M. Taillefer, *Angew. Chem., Int. Ed.*, 2009, **48**, 6954–6971.
8 L. M. Huffman, A. Casitas, M. Font, M. Canta, M. Costas, X. Ribas and S. S. Stahl, *Chem. Eur. J.*, 2011, DOI: 10.1002/ chem.201100608.
9 X. Ribas, C. Calle, A. Poater, A. Casitas, L. Gómez, R. Xifra, T. Parella, J. Benet-Buchholz, A. Schweiger, G. Mitrikas, M. Solà, A. Llobet and T. D. P. Stack, *J. Am. Chem. Soc.*, 2010, **132**, 12299–12306.
10 X. Ribas, D. A. Jackson, B. Donnadieu, J. Mahía, T. Parella, R. Xifra, B. Hedman, K. O. Hodgson, A. Llobet and T. D. P. Stack, *Angew. Chem., Int. Ed.*, 2002, **41**, 2991–2994.
11 M. Albrecht and G. van Koten, *Angew. Chem., Int. Ed.*, 2001, **40**, 3750–3781.
12 R. H. Crabtree, *Science*, 2010, **330**, 455–456.
13 T. A. Neubecker, S. T. Kirksey, K. L. Chellappa and D. W. Margerum, *Inorg. Chem.*, 1979, **18**, 444–448.
14 S. T. Kirksey and D. W. Margerum, *Inorg. Chem.*, 1979, **18**, 966–970.
15 The same violet species **3** is obtained by reaction of **2** with sodium acetate, no deprotonation is achieved by treating aryl–Cu^{III}-halide species with base due to the enhanced stability (see ref. 8); furthermore, the addition of one equiv. of Cl^{-} to **3** forms quenches inmediately its violet color and forms aryl–Cu^{III}-Cl (see ref. 22).
16 C. P. Keijzers, G. F. M. Paulussen and E. D. Boer, *Mol. Phys.*, 1975, **29**, 973–1006.
17 J. E. Roberts, T. G. Brown, B. M. Hoffman and J. Peisach, *J. Am. Chem. Soc.*, 1980, **102**, 825–829.
18 A. Romero, C. W. Hoitink, H. Nar, R. Huber, A. Messerschmidt and G. W. Canters, *J. Mol. Biol.*, 1993, **229**, 1007–1021.
19 S. D. George, L. Basumallick, R. K. Szilagyi, D. W. Randall, M. G. Hill, A. M. Nersissian, J. S. Valentine, B. Hedman, K. O. Hodgson and E. I. Solomon, *J. Am. Chem. Soc.*, 2003, **125**, 11314–11328.
20 L. M. Huffman and S. S. Stahl, *J. Am. Chem. Soc.*, 2008, **130**, 9196–9197.
21 A. E. King, L. M. Huffman, A. Casitas, M. Costas, X. Ribas and S. S. Stahl, *J. Am. Chem. Soc.*, 2010, **132**, 12068–12073.
22 A. Casitas, A. E. King, T. Parella, M. Costas, S. S. Stahl and X. Ribas, *Chem. Sci.*, 2010, **1**, 326–330.
23 H.-Z. Yu, Y.-Y. Jiang, Y. Fu and L. Liu, *J. Am. Chem. Soc.*, 2010, **132**, 18078–18091.
24 G. O. Jones, P. Liu, K. N. Houk and S. L. Buchwald, *J. Am. Chem. Soc.*, 2010, **132**, 6205–6213.